3. Physical Effects of Climate Change

Increases in atmospheric carbon dioxide levels have resulted in warmer air and water temperatures with cascading effects on winds, precipitation, sea level, and ocean circulation. In turn, these changes can interact to produce consequences such as increased flooding and erosion due to increased precipitation and sea level rise. In addition, increased atmospheric CO_2 has altered ocean chemistry. This chapter outlines the changes in the physical ocean-atmosphere environment off north-central California that are anticipated to occur as a result of global climate change. As an additional resource, the United States Global Climate Change Research Program published "Global Climate Change Impacts in the United States" (2009), which contains scientific assessments of global climate change impacts specific to coastal regions.

In addition to anthropogenic trends in the climate of the northeast Pacific Ocean, significant natural climate fluctuations occur on interannual, interdecadal, and multi decadal time scales. It is important to recognize this natural variability in identifying long-term trends in ocean and atmospheric properties. It is anticipated that anthropogenic climate change is likely to alter this natural variability as well as annual average conditions. The combination of climate change trends with this natural variability may create new extreme conditions. For example, the high waves during El Niño events will be more extreme when combined with the climate-change trend of increased wave height (see 3.3.2 Waves and 3.4 Sea Level Rise). Likewise, in the positive phase of the Pacific Decadal Oscillation (PDO), climate-change warming may be accelerated along with enhanced rainfall, runoff, wave activity, and erosion but with overall reduced upwelling. During the negative phase, in contrast, climate-change warming effects will be slowed. Thus expected impacts of climate change could be delayed many years during the negative phase of the PDO and accelerated during the positive phase.

The following modes of variability (natural climate fluctuations) are well documented for the ocean and atmosphere off California:

El Niño Southern Oscillation (ENSO) – Easterly trade winds and the piling up of warmer waters in the western Pacific Ocean relax during the positive phase of ENSO (termed El Niño) and typically occurs every three to seven years (Rasmussen and Wallace 1983; Fig. 3.1). This results in greater sea surface temperatures in the eastern Pacific and a deeper surface mixed layer, which results in upwelling of warm low-nutrient waters and a reduction in productivity that is confined to a narrow band along the U.S. west coast. El Niño has a marked negative effect on ecosystem productivity (Barber and Chavez 1983). During strong El Niño events, storm tracks have a more westerly approach (Seymour et al 1984) and are associated with greater wave height and precipitation (Storlazzi and Griggs 2000). The opposing phase of El Niño is termed La Niña and is mostly characterized by the opposite effects of El Niño.

Pacific Decadal Oscillation (PDO) – The PDO describes a longer-term fluctuation in ocean climate that changes state approximately every 20-40 years (Trenberth 1990; Trenberth and Hurell 1994; Fig. 3.1). During the "warm" phase of PDO, warmer ocean temperatures are observed in the California Current, while lower sea surface temperatures are found in the northwest Pacific. The "cool" phase of PDO exhibits the opposite pattern. In contrast to ENSO, where a coupled ocean-atmosphere response has been well documented as the mechanism, the dynamics underlying the PDO are not well understood (Mantua and Hare 2002).

North Pacific Gyre Oscillation (NPGO) – Fluctuations in sea surface height and temperature data across the northeastern Pacific are well described by the NPGO in combination with the PDO (Di Lorenzo et al. 2008). While the PDO is the dominant signal in physical parameters such as temperature and sea level, the NPGO correlates well with decadal scale fluctuations in salinity, nutrient concentrations and chlorophyll. This suggests that the NPGO may best describe the relationship between nutrient fluxes and ecosystem productivity (Di Lorenzo et al. 2008; 2009).

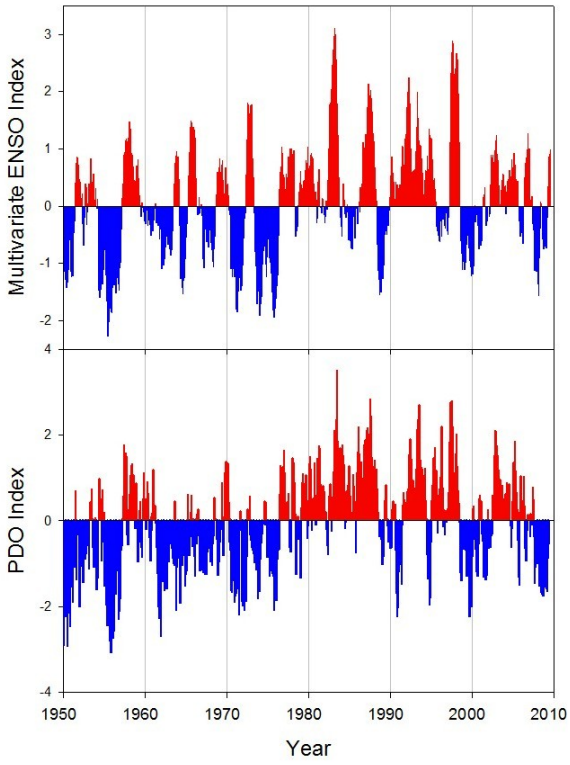

Figure 3.1. *Time series of the Multivariate ENSO Index (top) and the PDO (bottom). Positive values are shaded red and negative values are shaded blue. Derived from N.Mantua time series: http://jisao.washington.edu/pdo/PDO.latest.*

3.1 Atmosphere

During spring and summer, winds blow strongly and persistently along the California coast towards the equator. The wind speed diminishes during fall and in the winter the average alongshore winds are near zero, in spite of strong southerly (northward directed) winds during winter storms (Dorman and Winant 1995). These winds are due to a large-scale land-ocean pressure gradient and their strength is governed by the position of the North Pacific High Pressure system and the strength of the continental thermal low-pressure system. Winds tend to be weaker closer to the coast, owing to the effects of friction and topography. This pattern of wind shear (known as wind stress curl) extends upwelling effects further offshore. Topographic features like Point Arena lead to stronger local winds (Winant and Dorman 1997), partly explaining the upwelling maximum observed at this headland in the northern portion of the study region. The North Pacific High also promotes the formation of the marine layer near coastal California. Descending air "caps" cold air that is formed near the cool ocean water resulting in a temperature "inversion" that subsequently forms the marine layer. In turn, the marine layer promotes the formation of fog and stratus clouds, with important effects on coastal temperature and solar radiation.

3.1.1 Wind

It has been proposed that the build-up of greenhouse gases will result in the enhancement of daytime heating and inhibition of nighttime cooling, leading to intensification of the continental thermal low-pressure system (Bakun 1990). This intensification will enhance the cross-shore pressure gradient and thus also enhance equatorward winds along the coast. Regional numerical models (Snyder et al. 2003, Auad et al. 2006) have found that increased global temperatures indeed lead to stronger wind stress along the California Coast, in particular during the summer-fall seasons in central California.

Alongshore wind time series in the region, from the 1940's to the 1990's, show that equatorward alongshore winds have increased in central California (Bakun 1990; Schwing and Mendelssohn 1997, Mendelssohn and Schwing 2002). Analysis of wind data from National Data Buoy Center (NDBC) buoys in the study region corroborate an enhancement in the alongshore winds between April and October from 1982 to 2007 (Garcia-Reyes and Largier 2010). Other upwelling regions similar to central California also appear to have experienced increased upwelling-favorable winds in the last decades (see 3.3.3,Coastal Upwelling; Bakun 1990; Mendelsson and Schwing 2002; McGregor et al. 2007). A similar pattern of coastal upwelling intensification has been observed along other eastern ocean margins that support ecosystems comparable to the California Current (Bakun 1990).

The time of year when the strong equatorward winds start, known as spring transition, has not changed consistently. However, the strong equatorward winds appear to be enhanced consistently during the summer and early fall, extending the normal wind season into the fall off central and northern California (Garcia-Reyes and Largier 2010), as projected by the numerical models (Snyder et al. 2003, Auad et al. 2006). North of 44° N, a trend towards a later spring transition and shorter upwelling season has been reported by Bograd et al. (2009).

A recent study by Lebassi et al. (2009) indicates that summer air temperatures at inland sites of California are warming while coastal valleys have actually cooled since the late 1940s. Results also show an increase in local onshore pressure gradients during the warm season, leading to the hypothesis that onshore movement of marine air is stronger (but see contrary evidence later in this section). This would imply a stronger sea breeze and most likely more extensive coastal cloudiness. The authors note that the higher elevations of the coastal mountains are warming while the coastal valleys are cooling, implying a stronger marine layer in coastal areas. A stronger marine layer would induce a stronger coastal wind jet moving from north to south and thus an increase in coastal upwelling. This in turn would lead to more frequent development of coastal stratus formation leading to positive feedback on the strength and persistence of the marine layer.

Scale Dependency of Climate Change: Air Temperature

Observed responses to climate change will show differences due to their spatial or temporal scale. For example, patterns of change at one spatial scale (e.g., the Pacific Ocean) may be very different than patterns at another spatial scale (e.g., the Farallon Islands). In other words, patterns *depend* on the spatial or temporal scale that is being examined. This "scale dependency" results in a cautionary approach by many scientists who thus do not generalize their results to larger or smaller scales without careful further study. In part, this is the rationale in referring to the anthropogenic forcing of world climate as "climate change" as opposed to "global warming". Warming refers to a specific process and direction of change at the global scale, whereas climate change refers to a broader suite of more complex changes in climate.

For example, a recent analysis of air temperature data at 253 California National Weather Stations further highlights the complexities of a changing climate. Lebassi et al. (2009) documented increased average air temperatures (0.23°C decade^{-1}) when analyzing all stations from 1950 – 2005. However, further analysis of the data by region indicated that low-elevation coastal areas actually cooled (-0.30°C decade^{-1}) and inland stations warmed (0.16° C decade^{-1}). Potential mechanisms for this may be the increase in upwelling (see above and 3.3.3 Coastal Upwelling) and/or a "reverse reaction" to warming in which increased temperature differentials between the land and ocean result in stronger sea breezes that lead to cooler air temperatures in coastal areas (Fig. 3.2). In summary, it should be clear that generalized statements for broad regions and long periods may not sufficiently characterize the complex response of a changing

3.1.2 Storms

Graham and Diaz (2001) observed an increase in extreme winds associated with North Pacific winter cyclones (i.e., extra-tropical cyclones) since 1948, due to an increase in deep cyclone[1] frequency and intensity. The authors report a 50% increase in the frequency of deep cyclones and 10-15% increase in winds. McCabe et al. (2001) corroborate the finding of increased intensity at both high (60-90°N) and mid-latitudes (30-60°N), but find a decrease in the frequency of cyclones at mid-latitudes while frequency does increase at high latitudes. This relative increase of cyclone frequency at high latitudes suggests a poleward shift of storm tracks (Trenberth et al. 2007).

North Pacific winter cyclones play an important role in increasing precipitation, generating large waves and raising coastal sea levels (wind-driven storm surge). Bromirski et al. (2003) studied non-tidal sea level residuals from the San Francisco tide gauge between 1858 and 2000. Their results show a significant increase in intense winter storms since 1950. Further, Wang and Swail (2001) report an increase in the largest waves (see 3.3.2 Waves), which they also attribute to an increase in the occurrence of storms. These results are consistent with reports indicating that 1-in-100 year coastal flooding events are likely to occur more frequently, with a probability of 1-in-10 years in the future (DWR 2006).

[1] Generally, stronger cyclones have lower pressure. In this context, the authors defined a "deep cyclone" as one that has a minimum central pressure less than 975 hectopascals (Graham and Diaz 2001).

3.1.3 Clouds

During late spring and into early fall, the California coastline is quite often shrouded in marine stratus (low lying clouds that do not contact the ground) and/or fog (clouds that come in contact with the ground and reduce visibility). This is a very important part of the long-term climate of coastal California because the formation of stratus and fog can significantly reduce solar insolation and temperature on the coast. Recently, Johnstone and Dawson (2010) analyzed hourly records of cloud ceiling height from airports at Arcata and Monterey, California, going back to 1951. Since this time, there was evidence of a decreasing trend in fog frequency (-2.2% per decade in relative terms). Furthermore, when this data was analyzed with a larger and older temperature dataset they infer a decline in fog frequency since the beginning of the 20th century (Fig. 3.2). The authors speculate that a gradual retraction of the North Pacific High could contribute to decreased formation of the marine layer with subsequent declines in fog and increases in coastal temperature

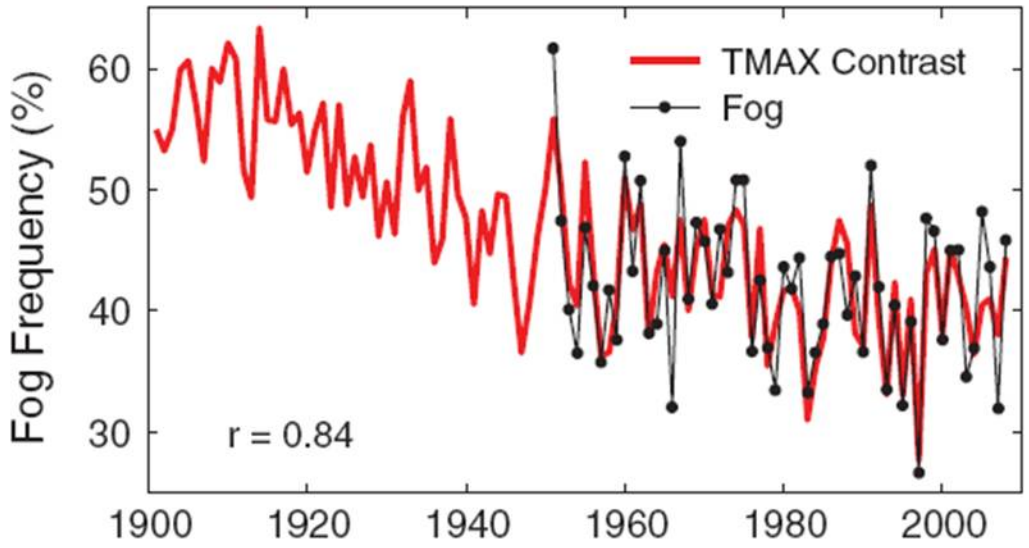

Figure 3.2. Fog frequency (black line) and T_{MAX} contrast (red line). The T_{MAX} contrast is a statistical proxy for 114 summer temperature records. Because T_{MAX} is correlated with the existing fog frequency dataset, the authors infer a decline in overall fog frequency over the 20th century. *Adapted from Johnstone and Dawson (2010). Copyright (2010) National Academy of Sciences, U.S.A.*

3.2 Precipitation and Land Runoff

During the dry months in California, the flow from the Sacramento and San Joaquin Rivers to San Francisco Bay and the ocean is primarily due to snowmelt from the snowpack covering the Sierra Nevada range. This snowpack acts as a natural reservoir, delaying runoff from winter precipitation (Kiparsky and Gleick 2005). Although precipitation and runoff records from 1900 are the primary source for planning purposes, the past 200 years have consistently been wet when compared with longer-term records (Meko et al. 2001). Statistically significant trends indicate that both precipitation (Groisman et al. 2001, Mote et al. 2005) and monthly mean streamflow (Lettenmaier et al. 1994) in California have increased since the early 20th century. This is consistent with a 10% increase in precipitation for all of North America since 1910. Multiple studies report that the majority of the increase in runoff is accounted for by increases in extreme precipitation during single-day events (Groisman et al. 2001; Kundzewicz et al. 2007). Kim et al. (2002) and Snyder et al. (2002) used global climate models to show that precipitation

in California is likely to continue to increase, with the greatest change centered in northern California. However, using low and medium-high IPCC emissions scenarios and two global climate models, Cayan et al. (2008) see small to no effects of warming on precipitation. The authors also note that the GCMs do not offer fine enough spatial resolution to adequately describe the heterogenous character of California climate. Furthermore, analyses by California state climatologist James Goodridge suggest no trend in precipitation from 1890-2002 for the entire state (DWR 2006). When California is divided into three regions (northern, central, southern), a slight increase in precipitation is seen in northern California, as opposed to slight decreases for central and southern California. The marked differences in results among these studies may be due to differences in the period of analysis, the number and location of stations, and the region selected for analysis.

A warming-induced change in the timing of peak streamflow events is a consistent result among both historical observations and modeling efforts (Dettinger and Cayan 1995, Stewart et al. 2004, 2005). Rising temperatures will likely result in a retreat of snow cover and a decrease in the precipitation ratio of snowfall to rainfall in northern and central California (Knowles et al. 2004). In both modeling and observations this is seen as an increase in runoff during winter months, a decrease in runoff during spring and summer, and a higher annual peak runoff (Kiparsky and Gleick 2005). Additionally, recent studies suggest that heavy precipitation events will become more prevalent (Kundzewicz et al. 2007). This is supported by an increasing variability in precipitation (DWR 2006; Fig. 3.3).

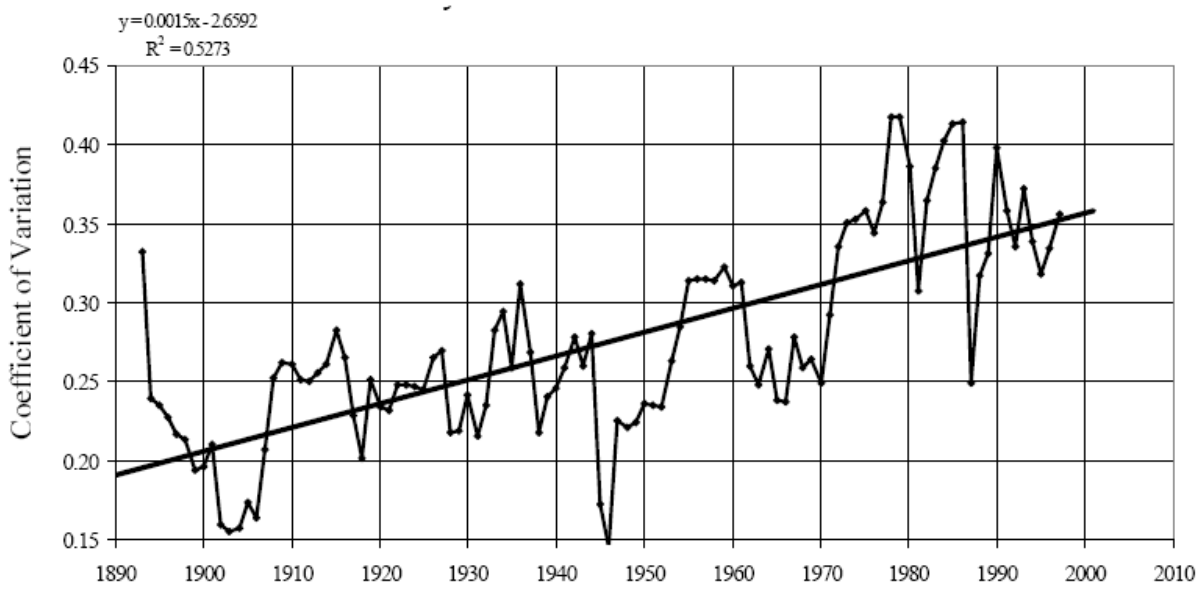

Figure 3.3. *Variation in precipitation over time in California. The solid line is the best-fit regression line. DWR (2006).*

The anticipated change in the occurrence of wildland fires associated with climate change (Westerling et al. 2006) may lead to enhanced runoff events. While relatively few studies have analyzed the effect of fires on runoff in California, those that have been conducted in similar regions have arrived at common results. The consensus is that fires increase runoff, sometimes by several orders of magnitude. Inbar et al. (1998) have shown that this is a result of lost vegetation coverage and changes to the soil properties resulting from the fire, while Johansen et al. (2001) show that total runoff volume after a fire is positively correlated with the percent of

the landscape covered by bare soil created during the event. Johansen et al. (2001) also show that the intensity of the fire strongly influences the eventual runoff rates, with low-intensity fires producing the least subsequent runoff volumes. In all studies, post-fire sediment yields also increased dramatically, in many cases by a higher proportion than that of runoff.

In summary, it is difficult to interpret trends in the historical record of precipitation as the results are highly dependent on the methodology used. Available evidence does suggest an increased frequency of extreme winter precipitation events in northern California, and a more rapid spring melting of snowpack (DWR 2006). This will lead to a shorter, more intense period of river flow and freshwater discharge in winter and spring (Dettinger and Cayan 1995, Cayan et al. 2001). In turn, this will greatly alter estuarine circulation patterns, riverine plume formation and coastal stratification and mixing (see 3.3.4 Estuarine Circulation and 3.6.3 Salinity), as well as the seasonal timing of the transport of materials and organisms to the ocean.

3.3 Ocean Currents and Waves

The movement of water in the ocean is driven by winds and differences in water density due to temperature and salinity. All of these factors are expected to change with the changing global and regional climate. In turn, changes in water movement will alter the transport of sediment, nutrients, plankton, contaminants and other water-borne material. The California Current is the eastern arm of the North Pacific Gyre (Fig. 3.4), which is largely driven by the winds that blow clockwise around the large high-pressure cell known as the Pacific High. The Pacific High strengthens and expands north in the northern summer and dominates west-coast winds from March through September. These northerly winds drive offshore transport of surface waters and upwelling of cold, deep, nutrient-rich waters along the coast. In addition to this larger scale wind-driven circulation are smaller density-driven flow features within or associated with estuaries (see 3.3.4 Estuarine Circulation) and the incessant action of waves on the shoreline (see 3.3.2 Waves).

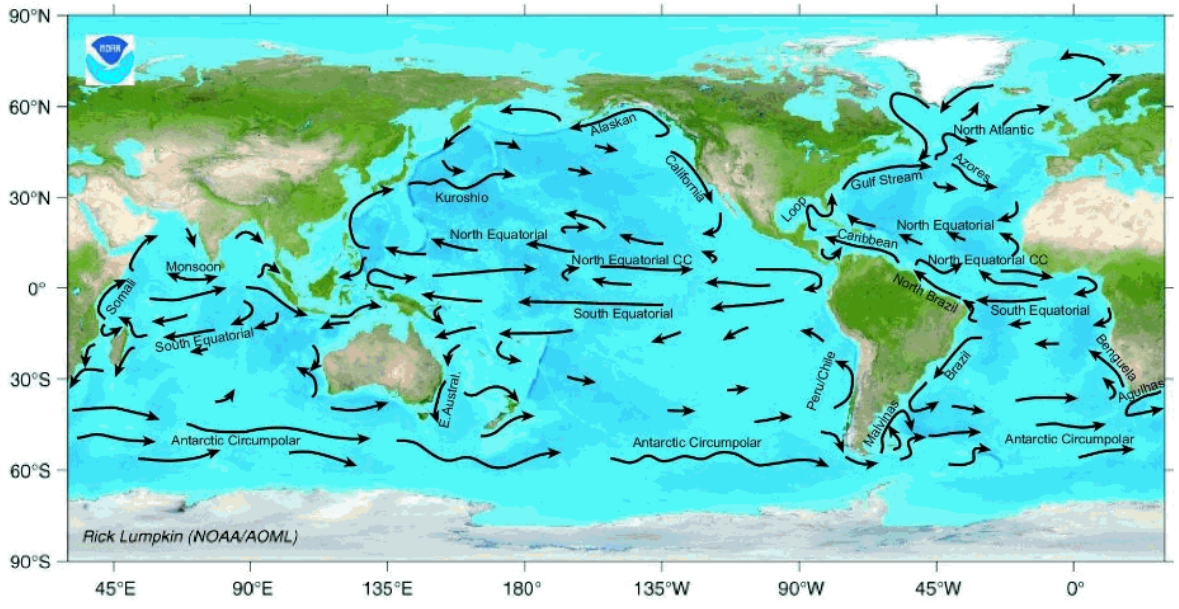

Figure 3.4. *World map showing the major ocean currents. The California current is the cold return current of the North Pacific Gyre moving south along the West Coast. Courtesy Rick Lumpkin, NOAA/AOML.*

3.3.1 Ocean Circulation

The circulation of the California Current, and the general upper ocean circulation for the North Pacific, is controlled by the North Pacific High pressure center off California and the Aleutian Low pressure cell near Alaska. A strong North Pacific High and weak Aleutian Low lead to enhanced southward transport in the California Current, cool surface waters and reduced stratification in addition to strong upwelling along the coast. These changes in ocean transport are known to affect the entire California Current Ecosystem (CCE), particularly the northern portion. However, the circulation of the North Pacific subtropical gyre combines with regional and local upwelling and advection to create a complex coastal circulation pattern for which future climate related changes have not been addressed adequately. Global-scale IPCC climate assessments do not address the effects of global climate change on ocean circulation satisfactorily and no attempt is made to assess changes in ocean circulation at the regional scale. One of the complexities of these projections is that natural interannual/interdecadal variations in ocean circulation can exceed the magnitudes expected due to long-term anthropogenic climate change (McPhaden and Zhang 2004). Long-term records of ocean circulation are needed to discern climate-change trends from fluctuations.

Decadal variations in regional transport patterns and water mass characteristics such as salinity, nutrients, and chlorophyll are linked to shifts in regional and large-scale circulation characterized by patterns such as the PDO and NPGO (DiLorenzo et al. 2008). Basin-scale adjustments in the subtropical gyre (e.g., NPGO) due to changing global wind stress patterns are thought to be a principal factor in these decadal fluctuations within the CCE, and can explain variations in regional water mass characteristics and related biological variables that are not correlated with surface indicators such as the PDO. A regime shift in the 1970s to a positive PDO state (warm CCE) accelerated eastward transport in the North Pacific Current (area annotated as West Wind Drift in Figure 3.5) and produced more subtropical source water for the CCE (Parrish et al. 2000).

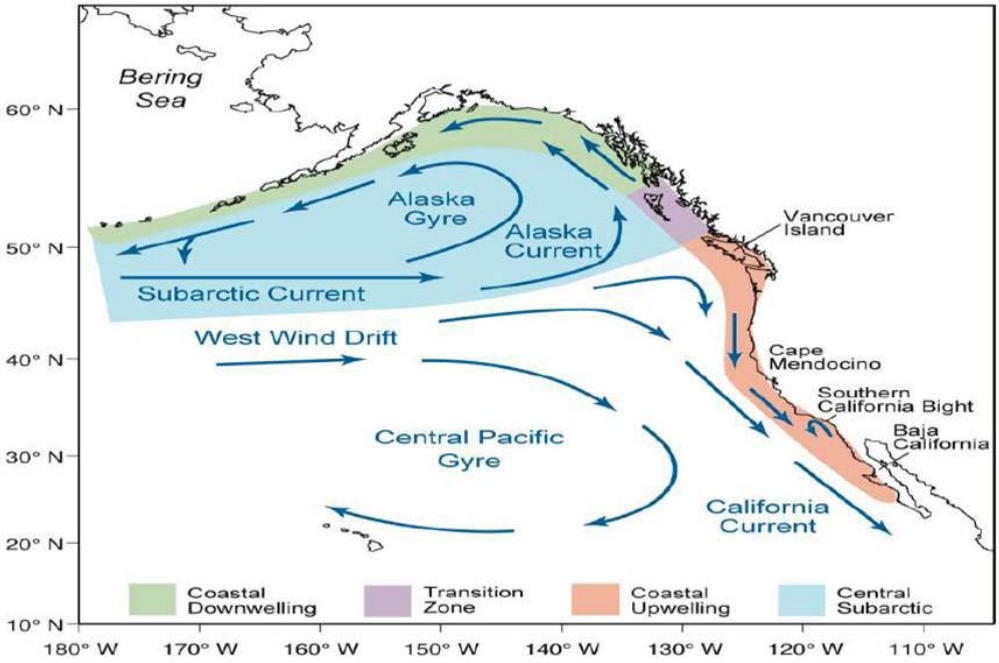

Figure 3.5. *Map showing the locations of the major currents in proximity to the study region. J.A. Barth (OSU, 2007).*

Some climate models suggest that global warming will weaken atmospheric circulation (Meehl and Teng 2007; Vecchi and Soden 2007), which could lead to a state in the North Pacific more like that during El Niños, along with a generally weaker southward flow of the California Current. The complexity of near-coastal circulation contributes to fronts and eddies that are important habitat features for many organisms, and corresponds to the speed of the subtropical gyre (Logerwell et al. 2003). It is thought that a stronger gyre will increase the southward transport of the California Current, creating more wind shear and a more complex circulation field.

3.3.2 Waves

Waves are a product of both local and distant processes. Large extra-tropical cyclones in the North Pacific send long-period swell towards the California coast between November and March, generating significant wave heights that occasionally exceed 8 m (Allan and Komar 2000). Significant wave height (H_s, defined as the average height of the highest third of measured waves) may reflect either these seasonal changes in swell wave generation or the intensity of the locally generated wave field. Short period (T_s < 10 s) waves are generated by local winds, and vary in height throughout the year. In summer, the development of the North Pacific High leads to strong northerly winds along the California coast that generates waves with smaller heights and shorter periods (Wingfield and Storlazzi 2007). Interannual differences in the wave field off California, especially north of the Golden Gate Bridge, are extremely responsive to climate variations such as ENSO (e.g., Seymour 1998; Allan and Komar 2000).

Figure 3.6. *Wave breaking at Maverick's, Half Moon Bay, CA. Josh Pederson / SIMoN NOAA.*

Installation of a buoy network along the US Pacific Coast in the 1980s, as well as a wealth of voluntary observer ship data, have allowed for comparative analyses of multiple phenomena that affect the California wave climate. Available data suggests that wave heights are increasing with latitude along the Pacific coast, with the greatest increases (>2 cm year^{-1}) occurring off the coasts of Washington and Oregon (Allan and Komar 2006; Fig. 3.7). Northern California's waves have increased less so, by an average rate of about 1.5-2 cm yr^{-1}, based on measurements from the NDBC Point Arena Buoy (# 46014). Increases for central California (Half Moon Bay #46012) are not statistically significant (Wingfield and Storlazzi 2007). These trends are verified by an extensive dataset from 1950-2002 (Gulev and Grigorieva 2004; 2006). This change in mean wave height is largely attributable to a disproportionate increase in peak storm waves relative to average waves (Wang and Swail 2001; Menendez et al. 2008).

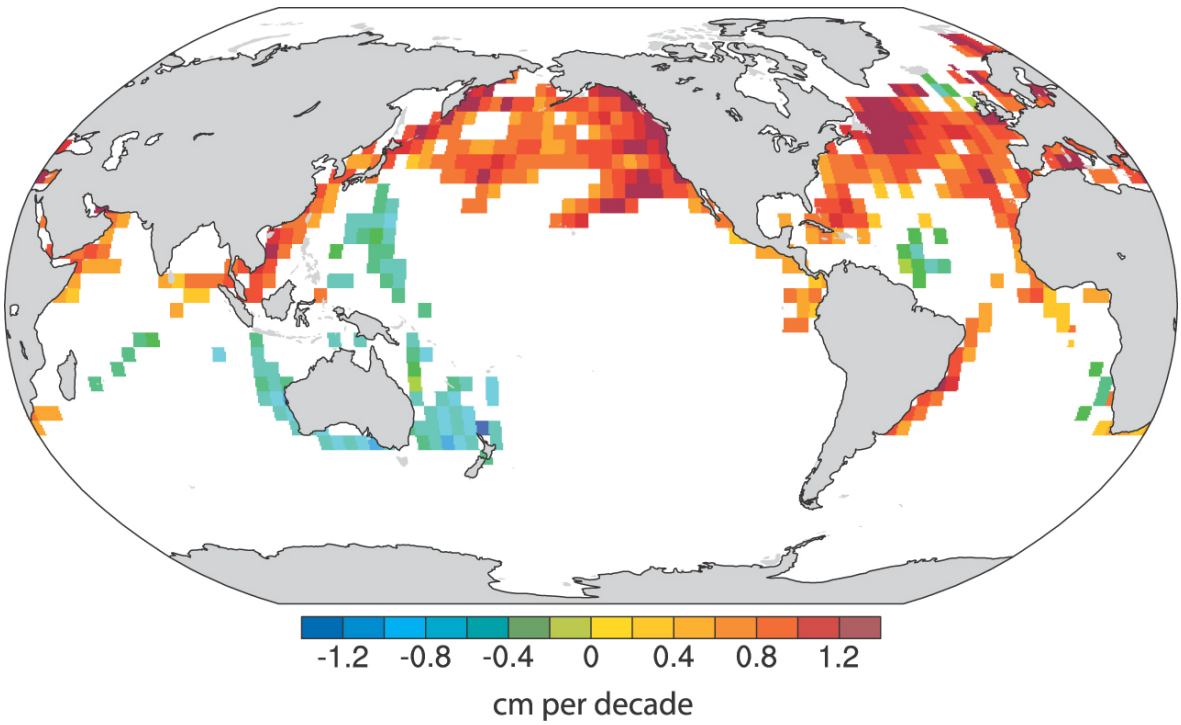

Figure 3.7. *Estimates of linear trends in significant wave height (cm per decade) for regions along the major ship routes of the global ocean for 1950 to 2002. Trends are shown only for locations where they are significant at the 5% level. Adapted from Gulev and Grigorieva (2004). IPCC.*

Observed changes in the regional wave climate are typically attributed to large-scale climatic changes in the central Pacific Ocean. Observed increases in sea surface temperatures in the Pacific could be responsible for the simultaneous increase in average wave heights (Graham and Diaz 2001), while the roles of the Eastern Pacific Teleconnectic Pattern (Allan and Komar 2000) and the difference between the Hawaiian high and the Aleutian low pressure zones have also been discussed (Wang and Swail 2001). Large-scale phenomena such as ENSO have also been shown to have dramatic effects on the California wave climate (e.g., Gulev and Grigorieva 2006; Wingfield and Storlazzi 2007). El Niño events shift the subtropical jet responsible for bringing storm systems to the California coast to a more southerly approach angle, which increases storm magnitude (Allan and Komar 2000; Storlazzi and Griggs 2000). Both El Niño and La Niña events tend to bring large waves to California, although El Niños are associated with the highest wave heights (Seymour 1998; Allan and Komar 2000; 2006). Both the ENSO phenomenon and the observed long-term increase in wave heights (particularly extreme wave heights) pose significant risks. Since El Niño events typically bring the largest recorded waves (Seymour 1998) and occur in late winter when most beaches are at their narrowest width, they are often the cause for the majority of coastal erosion, flooding, and property loss (Storlazzi and Griggs 2000; Wingfield and Storlazzi 2007).

The PDO also plays an important role in wave climate by moderating or increasing the intensity of El Niños and by further shifting the subtropical jet stream and affecting wave directionality (Bromirski et al. 2005; Adams et al. 2008). Changes in wave forcing during both PDO and ENSO events cause dramatic changes in wave direction which can expose normally sheltered beaches to dramatic erosion (Adams et al. 2008), or serve to rotate segments of sandy shoreline

from the south to the north, exposing the southerly ends of littoral cells to increased erosion such as in Pacifica, CA (Sallenger et al. 2002).

Available evidence suggests that significant wave height is increasing, particularly for northern California. These waves may also have greater impacts on coastal erosion, as El Niño conditions tend to modify the approach (more southerly) resulting in greater wave impact. If waves coincide with high tides they will also have a greater impact on erosional processes. Monitoring the intensity and direction of waves is important for biological communities because waves play a large role in structuring nearshore subtidal and intertidal marine communities (see 6.4 Sandy Beach Habitat, 6.5 Rocky Intertidal Habitat, and 6.6 Nearshore Subtidal Habitat). In intertidal habitat, wave forces affect organisms that are attached to or interacting with the substrate. In addition, the distribution of subtidal algal populations (e.g., kelps) is in large part determined by wave exposure (see 5.2 Macroalgae and Plants). Sub-tidal and intertidal ecological communities can also be affected by wave-driven abrasion of sediment (Storlazzi et al 2007). Waves can also influence sediment transport, the morphology of estuary mouths (see 3.3.4 Estuarine Circulation), and patterns of inundation (see 3.4 Sea Level Rise and 3.5 Coastal Erosion).

3.3.3 Coastal Upwelling

Wind-driven coastal upwelling delivers cold nutrient-rich waters to the near-surface light-filled zone, providing the foundation of the high biological productivity off California and within the study region (Fig. 3.8). Coastal upwelling results from the offshore transport of near-surface water due to alongshore winds from the north and the influence of the earth's rotation (known as Ekman transport). This water is replaced with cold, salty, nutrient-rich water from depths below.

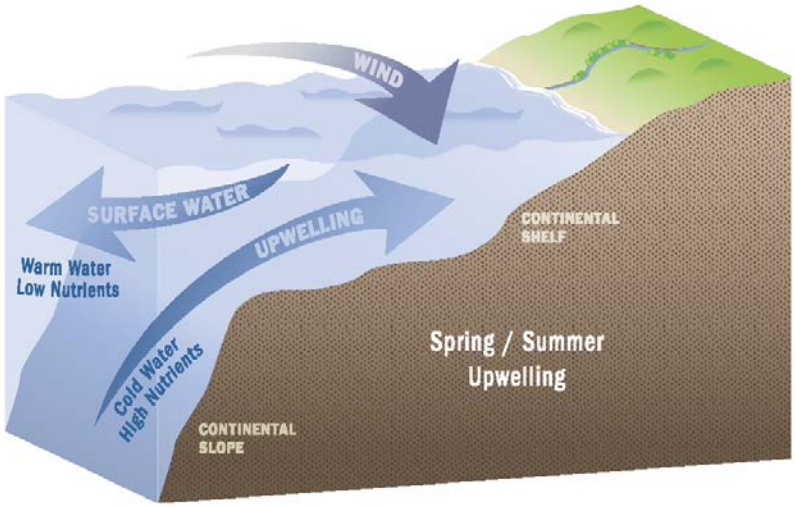

Figure 3.8. *Spring/Summer upwelling diagram. GFNMS.*

In addition to this vertical circulation and the upward bending of isotherms towards the coast, there is a set-down or lowering of sea level of about 0.1-0.2 m during upwelling events. Further, this cross-shore sea level slope drives a strong southward upwelling jet over the shelf, with current speeds ten times more than that due to offshore Ekman transport – such that plankton and other water-borne material may move alongshore more so than offshore. When distant from active upwelling centers like Point Arena and along the coast north of Point Reyes, the newly upwelled waters warm while nutrients are consumed by developing phytoplankton blooms. In the lee of headlands like Point Reyes and Point Año Nuevo, the southward jet separates from the coast such that recirculation occurs and aging upwelled waters may be retained near the coast as they support phytoplankton blooms. The resultant surface lenses of warm water in northern Monterey Bay and the northern Gulf of Farallones region are observed to propagate northward along the coast during relaxation periods between upwelling events.

Earlier suggestions that global warming will lead to stronger alongshore winds and enhanced coastal upwelling (Bakun 1990) have been supported by recent model and observational studies. As the earth warms, the land is expected to heat up faster resulting in an increase in the land-sea temperature difference and in the associated land-sea pressure gradient that drives the northerly upwelling winds. Numerical simulations (Snyder et al. 2003; Auad et al. 2006) and measured wind time series (Mendelssohn and Schwing 2002; Garcia-Reyes and Largier 2010) describe enhanced alongshore winds in this region. Along with the increase in wind forcing, a cooling trend in sea surface temperature has been observed for the upwelling season (Bakun 1990; Mendelssohn and Schwing 2002; Garcia-Reyes and Largier 2010; Fig. 3.9). The implications of this for primary production, plankton dispersal, habitat changes, frontogenesis, and the occurrence of fog and low-level clouds are poorly known. Much depends on an understanding of how changes in the upwelling process will affect the larger California Current Ecosystem.

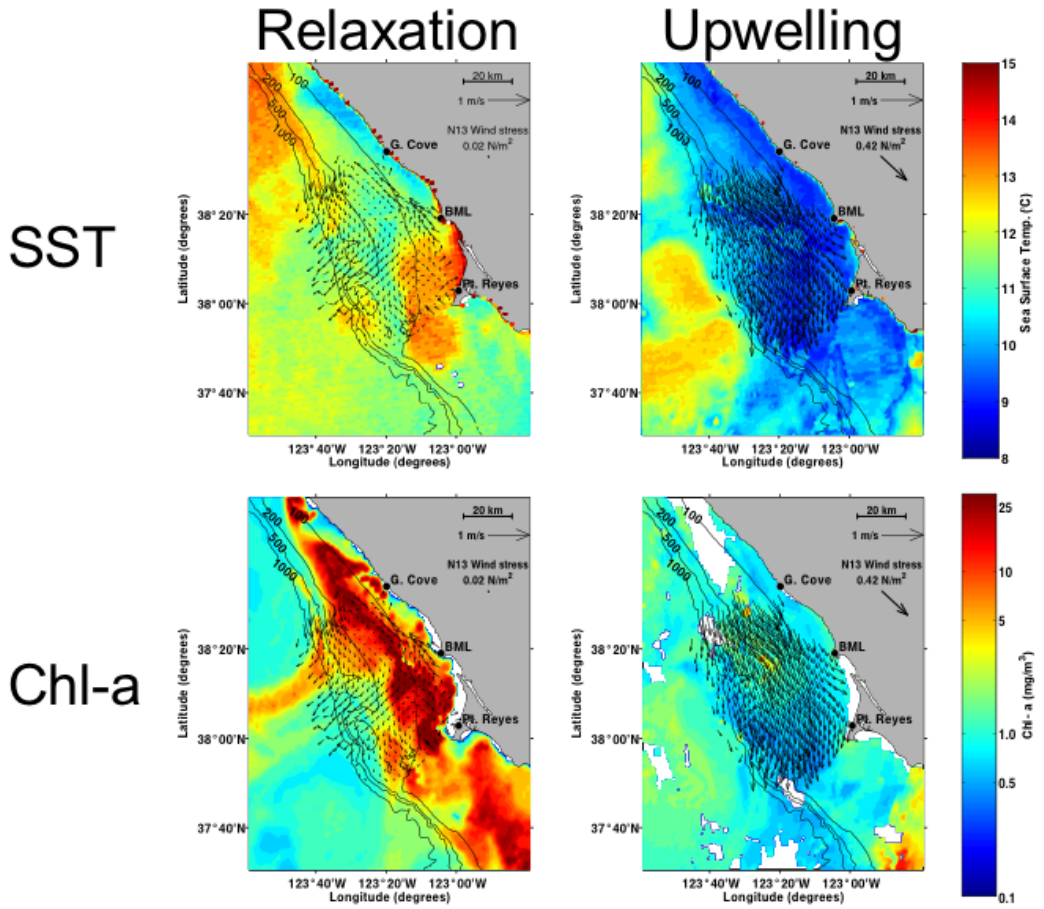

Figure 3.9. *Sea surface temperature (SST) and chlorophyll-a during upwelling and relaxation events. Largier et al. (2006).*

Cross-shore differences in ocean conditions are expected to arise with a warming of nearshore and enclosed bay waters, while enhanced upwelling can be expected to cool waters over the shelf. Further offshore, however, beyond the active upwelling due to a divergence in Ekman transport, an increase in surface heating is expected to exceed the cooling effects of increased upwelling. Offshore surface temperatures are expected to increase, along with an increase in

near-surface stratification and a decrease in the vertical mixing that replenishes near-surface nutrient levels and fuels primary production (Roemmich and McGowan 1995; Palacios et al. 2004.

The temporal variability in coastal upwelling is also very important to primary production and other critical ecological processes. Both the strength of upwelling winds and the nature of the synoptic variability in winds affect the amount of primary production available, and the amount delivered to coastal ecosystems rather than offshore ecosystems (Botsford et al. 2003; 2006). It is possible that enhanced upwelling will also be more persistent, resulting in less phytoplankton availability in coastal waters and a greater but more diffuse supply of phytoplankton to waters over the outer shelf and slope, while enhanced surface heating reduces phytoplankton availability due to increased stratification further offshore.

The seasonal timing of upwelling is expected to vary due to climate change and this will have numerous ecological impacts due to mismatches between the timing of upwelling-induced primary production and the less-variable seasonal phenology of higher trophic levels. While an anomalous late onset of upwelling winds in spring 2005 and 2006 had negative impacts on the coastal ecosystem (Kosro et al. 2006; Sydeman et al. 2006), there is no evidence of a trend towards a delay in the start of the upwelling season associated with climate change. However, an enhancement of upwelling in the late summer and fall and delayed end to the season has been noted in studies based on models and data analysis (Snyder et al. 2003; Garcia-Reyes and Largier 2010).

Finally, the consequences of upwelling will also vary from year-to-year due to interannual to interdecadal variability in the offshore thermocline depth – a phenomenon associated with climate fluctuations such as ENSO and NPGO, and may also exhibit a trend associated with climate change. When the thermocline is deeper, wind-driven coastal upwelling will bring an increased amount of lower nutrient waters from above the thermocline to the surface, as happens during El Niño events.

3.3.4 Estuarine Circulation

In addition to sea level rise, estuaries are expected to respond significantly to altered land runoff due to changes in precipitation and to changes in wave energy at the mouth. Secondary influences include changes in local winds as well as temperature (i.e., changes in heating). A significant increase in sea level is expected (see 3.4 Sea Level Rise), resulting in flooding of littoral marshes and low-lying lands, unless there is a concomitant elevation of the land surface due to flood-induced sedimentation. While tides are forced by gravitational effects of the sun and moon, and not expected to be altered by global climate change, rising sea level may alter how tides propagate into estuaries, altering the timing and extent of the tidal rise and fall of water levels. Significant climate-related changes in land runoff strength and timing are expected (see 3.2 Precipitation and Land Runoff), in addition to changes due to water management in each watershed. Changes in local waves (see 3.3.2 Waves) and winds are also expected as a result of global climate change, in turn giving rise to changes in coastal currents that determine the fate of estuary outflow plumes.

Estuaries are characterized by the intrusion of salty seawater into basins or channels that carry freshwater runoff from land to sea. Within the estuary, waters are typically stratified with a low-

salinity layer overlying a high-salinity layer. By averaging tidal motion into and out of an estuary, "estuarine circulation" is observed, comprised of a seaward flow of the upper, low-salinity layer and a landward flow of the lower, high-salinity layer. The outflowing upper layer entrains high-salinity water from below, completing a conveyor-belt-like circulation for seawater into and back out of the estuary. This mixture of freshwater and seawater then exits the estuary as a stratified plume that spreads offshore and alongshore, with the fate of these plume waters determined by wave, wind, tide, buoyancy, and coastal currents.

The study region is influenced by and/or includes three types of estuaries: (i) San Francisco Bay and the tributary estuary system known as the Delta; (ii) semi-enclosed bays, e.g., Tomales Bay, Drakes Bay, Bolinas Lagoon, Bodega Harbor, with tributary estuaries; and (iii) drowned river valley and bar-built estuaries on the Gualala River, Russian Gulch, Russian River, Salmon Creek, Cheney Gulch, Estero Americano, Estero de San Antonio, Walker Creek, Lagunitas Creek, Pine Gulch Creek, Geronimo Creek, Waddell Creek, Scott Creek, Pescadero Creek, and smaller creeks/gulches. All of these have a role in providing coupled habitat or in affecting study region environments through runoff plumes.

The semi-enclosed bays exhibit estuarine circulation during the wet Mediterranean-climate winters, but behave as "low-inflow estuaries" in summer (Largier et al. 1997), with warm, salty waters and weak or no stratification due to thermal effects. Cold, upwelled waters may intrude at depth in the outer estuary, but salinity stratification is only observed in the small tributary estuaries, e.g., in the Lagunitas Creek estuary channel at the landward end of Tomales Bay (Abe 2008). The residence time of waters in these basins is long during the long dry summers (e.g., 2-3 months in Tomales Bay) and controlled by tidal action (Largier et al. 1997).

Sea level rise and reduced freshwater inflow are expected to result in landward movement of saline waters (unless the estuary mouth closes before the seasonal decrease in river flow). Specifically, increased salinity intrusion is expected in San Francisco Bay in response to decreased snowmelt flows in spring. In estuaries fed by coastal watersheds, concern is more related to winter periods as many estuary mouths close in summer. However, the mouths of the tributary estuaries in the semi-enclosed bays do not close (e.g., Lagunitas Creek) and the combination of rising sea level and decreased summer runoff is expected to result in significant intrusion of saline waters, affecting local water resources.

Strong runoff is key in flushing estuary basins, but also may scour bottom sediments and erode estuary banks. Where banks are compromised (due to human activities), extreme flow events will lead to major changes in morphology and disruption of socio-economic activities. Increases in storm intensity and rain intensity would lead to more frequent and more severe flooding of low-lying lands, requiring decisions on the merits of flood control versus natural functioning and system adaptation. Flooding risk will also increase due to both past and future rise in sea level.

River flow working with tidal flow is also important in maintaining an open mouth in bar-built estuaries, removing sediment deposited in the mouth by wave action. The seasonal cycle of estuary mouth closure will change in response to changes in river flow, tidal prism changes due to sea level rise, and changes in wave energy. If river flow is enhanced (stronger and more persistent) or wave forcing becomes weaker, then the mouth will remain open longer – or, alternatively the mouth will tend to close for weaker river flow and/or stronger waves. In

addition to changes in intensity, changes in the relative seasonal timing of river flow and wave energy are important. If river flow continues later in spring, this may keep the mouth open beyond the time when waves are big enough to close an estuary – in which case that estuary could remain open much longer than previously (e.g., Behrens et al. 2008). Alternatively, if river flow decreases early, while waves are still large, the estuary will close much earlier than previously (and may prevent estuary-ocean migrations that typically occur in spring, e.g., smolts emigrating to the ocean). In the fall, if waves increase early while river and runoff is delayed, this would lead to fall closures or keep the mouth closed longer than previously (again preventing estuary-ocean migrations).

When estuaries are closed in summer, they function as a salt-stratified lake. The lower, high-salinity layer is trapped and may develop hypoxic or anoxic conditions (e.g., Russian River) and/or very high water temperatures (e.g., 34^{o}C in Salmon Creek, Largier et al. 2007). Longer closures may aggravate these conditions. When estuaries are open, there is a continual exchange of ocean and estuary waters – and a surface plume of estuarine water forms during ebb tides (or continuously during periods of strong river flow). This plume delivers biogenic material, sediment and contaminants to nearshore waters. The fate of these plume waters and their loading will change with climate-related changes in river flow, mouth condition, nearshore wave-forced currents, and offshore wind-forced currents.

When estuaries are open, there is a continual exchange of ocean and estuary waters – out on the ebb tide and in on the flood tide. During strong river flows, there may be continuous outflow. Whether these estuarine outflows are primarily aged ocean water or land runoff water, the outflow forms a distinct jet near the mouth that evolves into a stratified plume at greater distances from the source. This plume delivers biogenic material, sediment and contaminants to nearshore waters (and offshore waters in the case of larger outflows, such as San Francisco Bay and Russian River estuary). The fate of these plume waters and their loading will change with climate-related changes in outflow water density (due to salinity), wave-forced currents, winds and offshore currents (typically related to wind forcing).

The climate-related changes in estuary conditions that are of primary concern are: (i) changes in mouth closure timing and persistence, (ii) changes in degree and frequency of flooding, (iii) upstream salinity intrusion, and (iv) fate of estuary outflows. The extent of changes depends on the interacting drivers, specifically river flow rate, sea level rise, wave energy and wind-forced currents.

3.4 Sea Level Rise

Global sea level rise is a well-recognized result of global warming. Sea level is affected through two primary mechanisms – thermal expansion of ocean water and ice melt (IPCC 2007). However, large uncertainty exists in predicting sea level rise due to future melting of polar ice sheets. (Bell 2008). Global tide gauge data from 1870 to 2004 show a 19.5 centimeter (cm) rise in global sea level during this period (Church and White 2006). Between 1961 and 2003, global sea level rose at an average rate of 0.018 cm per year, with this rate increasing between 1993 and 2003 to about 0.31 cm per year (IPCC 2007). Vulnerability studies have utilized a medium-high emissions scenario for the California coast of 40 cm of sea level rise by 2050 and 140 cm by 2100, which was developed using the methodology of Rahmstorf (2007) and Cayan et al. (2008). Currently the state of California has adopted these projections for adaptation planning purposes

under the directive issued for sea level rise in Executive Order S-13-08. Therefore, these projections will be used for this document. However, it should be noted that a new analysis projects sea level rise of 75 to 190 cm by the year 2100 (Vermeer and Rahmstorf 2009).

The rate of sea level rise at a specific location is determined by tectonic movements, as well as the local wind and wave fields that are superimposed on top of global sea level rise. These factors are additive, and when combined, determine the relative sea level rise at that location. Since the study region is along an active margin, the role of tectonic uplift and subsidence are important in determining the relative rates of sea level rise. Along the study area, the San Gregorio, Hayward, and San Andreas Faults play important roles in determining the movement of the land. Because these faults generally slide next to each other (right lateral transform faults), the uplift and subsidence rates are lower than along the Pacific Northwest subduction zone north of Cape Mendocino. Uplift rates have been documented for marine terraces just south of the study region through Point Arena and show rather small rates of uplift ranging from 0.4 - 1.1 mm/yr (Prentice et al. 1999, Perg et al. 2001). When comparing these rates of uplift with a 100 year projected sea level rise of 1.4 m (~14 mm), the relative influence of this uplift is minor.

Local rates of sea level rise also vary in response to interanual/interdecadal fluctuations in wave and atmospheric circulations. El Niño events, storm surges, and strong onshore directed winds can raise sea levels up to 30 cm above predicted tides (Flick 1998, Bromirski et al. 2003). In addition, larger scale climate fluctuations, such as PDO, moderate or enhance El Niño conditions. Recent research shows that the sea surface elevations off of the central California coast have been suppressed in comparison to global averages (Ramp et al. 2009). The PDO has been implicated in this finding, but researchers also point out that this is a temporary cycle, that when it reverses, is likely to lead to local sea level rise rates higher than global averages (see box: Scale Dependency of Climate Change, Sea Level Rise).

Scale Dependency of Climate Change: Sea Level Rise

Global average sea level has been rising as indicated by reconstructed and direct data from the late 19th century to the early 21st century (Bindoff et al. 2007). However, it has become increasingly clear that the rate of sea level change is not consistent in space or time. Recent reanalysis of sea level data from the San Francisco tide gauge station (dating to the mid 19th century) corroborates rising sea level trends observed by other studies (Ramp et al. 2009). However, since 1997, sea level has actually been falling due to a phase shift of the Pacific Decadal Oscillation (PDO) to the "cool" state (Fig. 3.11). While the mechanism by which the PDO affects sea level requires further study, it is expected that a transition back to the warm state of the PDO will result in an accelerated rate of sea level rise (Ramp et al. 2009). Therefore, a different answer for sea level rise will be obtained depending on whether data is analyzed for 100 years or 10 years.

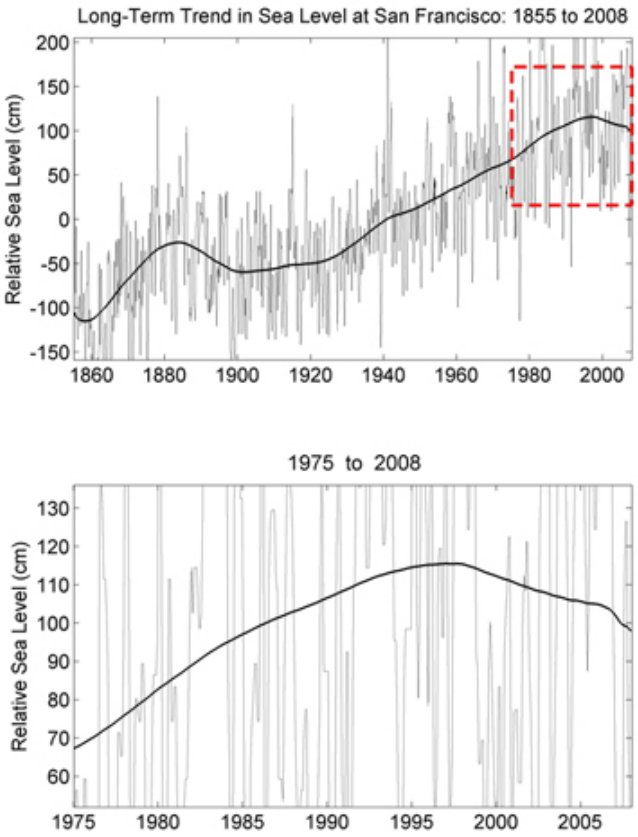

Figure 3.11. *Long-term trends in sea level at San Francisco, 1855 to 2008. The lower panel is an expansion from the upper panel. Adapted from Ramp et al. (2009).*

Sea level along the California coast has increased by about 15 cm over the past century (CEC, 2006). Locally, the San Francisco Bay Area has one of the longest recorded time series of sea level data in the United States. The San Francisco tidal gauge was installed in 1854, making it the oldest continually operating tidal observation station in the nation (NOAA/NOS 2008). The trend in sea level rise for the San Francisco Bay Area over the last century is approximately 2.01 millimeters per year which is equivalent to a change in ~0.66 feet (20.1 cm) over the last 100 years. (NOAA 2009; Fig. 3.12).

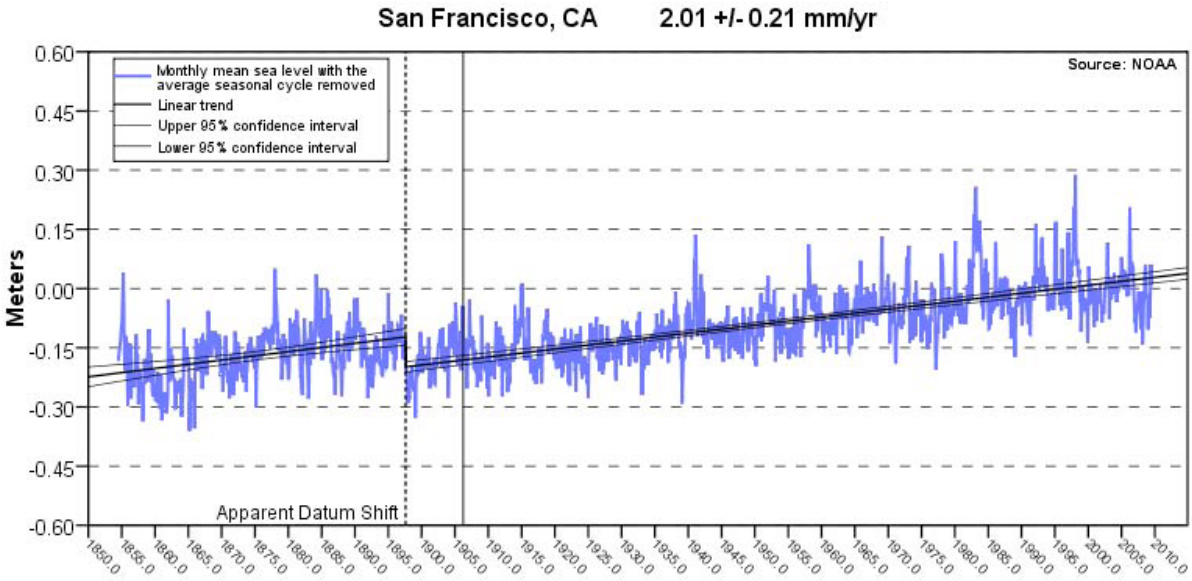

Figure 3.12. *The mean sea level trend for Gauge No. 9414290 San Francisco, CA is 2.01 millimeters/year with a 95% confidence interval of +/- 0.21 mm/yr based on monthly mean sea level data from 1897 to 2006, which is equivalent to a change of 0.66 feet (~20.1 cm) in 100 years. NOAA (2009).*

A primary impact of sea level rise on coastal habitats and communities is the increased likelihood and depth of coastal flooding. Coastal flood elevations can be determined by the sum of the constituent components including sea level rise, tides, storm surge, El Niño effect on temperature, and wave run-up. The sum of these components determines a total water level elevation, and as this increases, then the risk to coastal habitats and communities increases (see box: Extreme Conditions).

Extreme Conditions

Recent climate change studies have pointed out that the average frequency or average intensity of weather events may not change, as opposed to the occurrence of extreme conditions, which may increase. For example, median values of maximum wind speed in Atlantic tropical cyclones exhibit no trend from 1981-2006. In contrast, winds speeds in the 70th percentile and above have a positive linear trend, indicating an intensification of extreme cyclone wind speeds (Elsner et al. 2008). The importance of extreme events is highlighted when considering the effects of sea level rise on coastal infrastructure and development. When combined with high tides and storm surge, sea level rise can result in extreme flood events with significant economic consequences. Biological systems are not immune from extreme weather events as well. Indeed, often times average climate variables may not be as important as extreme events, which can have the largest effects on patterns of disturbance and mortality (Gaines and Denny 1993). Examples include large waves in the intertidal zone that dislodge organisms or extreme high temperatures that can result in mass mortality.

As the sea level rises, low-lying areas along the coast are more susceptible to flooding, including communities in Point Arena Cove, Bodega Bay, Bolinas, Tomales Bay and Stinson Beach (Fig. 3.13, and see http://www.pacinst.org/reports/sea_level_rise/hazlist.html for additional coastal flood and erosion hazard maps prepared by the Pacific Institute). Increased flooding will also affect the quality and functioning of a variety of coastal habitats such as wetlands, beaches, and dunes. Pendlelton et al. (2005) state, "Potential effects of sea level rise include shoreline erosion, saltwater intrusion into groundwater aquifers, inundation of wetlands and estuaries, and threats to cultural and historic resources as well as infrastructure". Sea level rise may also increase salinity in the San Francisco delta and other estuaries by as much as 9 practical salinity units (psu) (Knowles and Cayan, 2002), particularly if the period of seasonal low flow expands (Gleick 2000).

Figure 3.13. *Sea level rise flood risk in Tomales Bay. Additional maps are available for the California coast: http://www.pacinst.org/reports/sea_level_rise/hazlist.html*

3.5 Coastal Erosion

The majority of the sandy coast in this region is already classified as eroding (Bird 2000; Hapke et al. 2006; Hapke and Reid 2007; Patsch and Griggs 2007), partly as a result of human-induced changes in sediment supply and transport (Komar 1998). Coastal erosion may increase in the study region as a result of rising sea level, changing wave conditions, and storm frequency and intensity (PWA 2009a). Coastal habitats may be directly affected by these changes, or indirectly via human responses such as armoring, beach nourishment, or retreat. The extent of inland shoreline migration and loss of upland depends on geology and sediment supply, all of which affect wave exposure, shoreline elevation and resiliency. These are integral factors controlling habitat type and quality. While many of these factors vary on local scales, they are evaluated here on the broader regional scale.

Erosion: Erosion results from the interaction of coastal processes with coastal geological formations, although terrestrial processes such as elevated groundwater also influence it. Sea cliffs are more or less susceptible to erosion depending on the hardness of the geologic rock type. Other important factors that control erosion include the shoreline orientation, width of the protective beach, and wave exposure (Griggs et al. 2005). Shoreline change rates have been calculated for most of the study area by the U.S. Geological Survey (USGS) for sandy shorelines (Hapke et al. 2006) and seacliffs (Hapke and Reid 2007). The magnitude of coastal erosion is related to the coastal geomorpology. PWA (2009a) characterized the California coast into seacliffs and dunes, and developed a methodology intersecting the USGS shoreline change rates with the variability in geology and erosion rates alongshore to then predict future erosion hazards. Maps of these erosion hazard areas can be found at http://www.pacinst.org/reports/sea_level_rise/hazlist.html.

Most of the coastline in the study area is backed by seacliffs, with Mendocino County projected to lose the largest area of land to coastal erosion (Table 1). Dune erosion is thought to have the largest impact in Marin County (an estimated 2.6 km^2), with erosion of almost 9 km^2 for the dunes across the entire study area. Total erosion by 2100 is estimated to reach nearly 50 km^2 (PWA 2009a; Table 1). These areas of erosion are not uniform across each county within the study area and show a range of inland erosion distances (Table 2; PWA 2009a). Maximum erosion distances, occur along the dune backed stretches of coastline and can reach over 400 m in some areas (Table 2). These maps and values are an approximation and not intended to form the basis for site-specific actions, but rather to provide an overall estimate of the potential scale of vulnerability. For example, the estimated erosion may take longer than 100 years as a result of the delay between rapid sea level rise and erosion; it may take less if sea level rises faster than projected. Overall, an enhanced potential for coastal erosion in this region is expected, however these projections assume no human intervention.

Table 1. *Total erosion area (alongshore + acrossshore) with a 1.4 m sea-level rise, for counties intersecting the study region.*

County	Dune erosion miles^2 (km^2)	Cliff erosion miles^2 (km^2)	Total erosion miles^2 (km^2)
Marin	1.0 (2.6)	3.7 (9.6)	4.7 (12.2)
Mendocino	0.7 (1.9)	7.5 (19.4)	8.3 (21.5)
San Francisco	0.2 (0.6)	0.3 (0.8)	0.5 (1.4)
San Mateo	0.8 (2.1)	2.4 (6.2)	3.2 (8.3)
Sonoma	0.6 (1.6)	1.6 (4.1)	2.2 (5.7)
Total (study area)	**3.3 (8.8)**	**15.4 (40.1)**	**18.7 (48.9)**

Table 2. *Average and maximum inland erosion distance in 2100, for counties in the study region.*

County	Dune erosion		Cliff erosion	
	Average distance (m)	Maximum distance (m)	Average distance (m)	Maximum distance (m)
Marin	140	270	110	240
Mendocino	190	440	33	160
San Francisco	150	230	90	220
San Mateo	230	430	31	220
Sonoma	150	320	41	190
Average m (ft)	**172 (564)**	**338 (1,109)**	**61 (200)**	**206 (676)**

Sediment Supply: To understand the impact of changes in sediment supply it is important to understand the sediment budget (for a variety of grain sizes) at a "sediment-shed" scale that includes the watershed, coastal wetlands and the littoral cell (e.g., Revell et al. 2007). A littoral cell is a defined nearshore region, constrained by headlands and submarine canyons, in which a beach-sand budget can be constructed, including a variety of sources and sinks. If there is a surplus in this sediment budget then beaches tend to be wide and shoreline erosion is weak or non-existent. Alternatively, if there is a deficit in the sediment budget then beaches are usually narrow and erosion rates are significant. The following are the littoral cells within the study region that have been identified: Navarro, Russian River, Bodega Bay, Point Reyes, Drakes Bay, Bolinas Bay, San Francisco, and Santa Cruz (Habel and Armstrong 1978; Patsch and Griggs 2007).

Human alterations in the watersheds, such as dams and debris basins, trap sediments and also affect peak flow rates – reducing the sediment transport to the coast (Willis and Griggs 2003; Slagel and Griggs 2008). This reduced supply of sand and cobbles to the individual littoral cells, pushes them towards a deficit and greater potential for erosion, reducing the resiliency of the beaches and wetlands. For example, construction of the Coyote Valley and Warm Springs Dams

on the Russian River has reduced the annual supply of coarse-grained material by more than 30% (Slagel and Griggs 2008).

The traditional human response to coastal erosion for protection of houses and infrastructure has been to armor the coast with physical structures such as seawalls and rip-rap. Shoreline armoring fixes the backshore in position and as sea level rises; the beach becomes trapped between the ocean and the armoring. Known as passive erosion, this impact effectively drowns beaches reducing the recreational and habitat value of this ecosystem.

Changes in precipitation and sediment discharge (see 3.2 Precipitation and Land Runoff) may play an important role in altering coastal erosion. If most precipitation events occur in short heavy events as projected (Dettinger and Cayan; 1995; Cayan et al. 2001; Kundzewicz et al. 2007), then sediment discharge is thought to increase which may widen beaches and reduce coastal erosion in places. However, given the numerous sediment and water retention structures in the watersheds, the sediment and water discharge effect of these events may be reduced and thus have negligible effect on the shoreline. In addition to greatly affect the resiliency of wetlands and beaches, changes in the magnitude of river and sediment discharge will as also interact with sea level rise and affect coastal hazards such as flooding and storm erosion events.

3.6 Ocean Water Properties

Both changes in the wind-driven coastal upwelling process and changes in the flow of the California Current will affect local water properties, including nutrient delivery to the euphotic zone and the biological effectiveness of upwelling. Decreasing upwelling winds and/or increasing stratification would lead to upwelling of waters from shallower depths – in turn resulting in higher temperatures, lower salinity and lower nutrient concentrations. At the same time, decreases in California Current transport would lead to the upwelling of coastal waters containing relatively more nutrient-poor subtropical water, leading to lower primary production. Another consequence of weaker transport by the California Current would be lower levels of dissolved oxygen in coastal waters (Bograd et al. 2008), since subtropical water carries less dissolved oxygen (Stramma et al. 2008). During reduced southward flow, a shallow oxygen-deficient zone can develop, which reduces the depth of favorable habitat for many marine organisms (Chan et al. 2008). In addition, the source waters that feed the California Current affect the composition of the plankton community, which in part determine the condition of higher trophic organisms.

3.6.1 Temperature

Global oceans have increased in temperature by 0.10°C from 1961-2003 (IPCC 2007). Levitus et al. (2005) and Ishi et al. (2006) documented long-term increasing trends in temperature coupled with decadal variability using temperature profiles from surface waters to 700 m. A third analysis over a more recent time period is also in general agreement with these findings (Willis et al. 2004). Increases in ocean heat content account for more than 90% of the change in global heat content from 1961-2003 (IPCC 2007; Fig. 3.14). This is due to the greater heat capacity of water relative to other components of the global energy budget (e.g., glaciers, ice sheets, continents, and the atmosphere). This increase in temperature may have significant effects on water column structure (e.g., stratification), ocean circulation patterns, sea level rise, and other climate phenomena (e.g., cyclone formation).

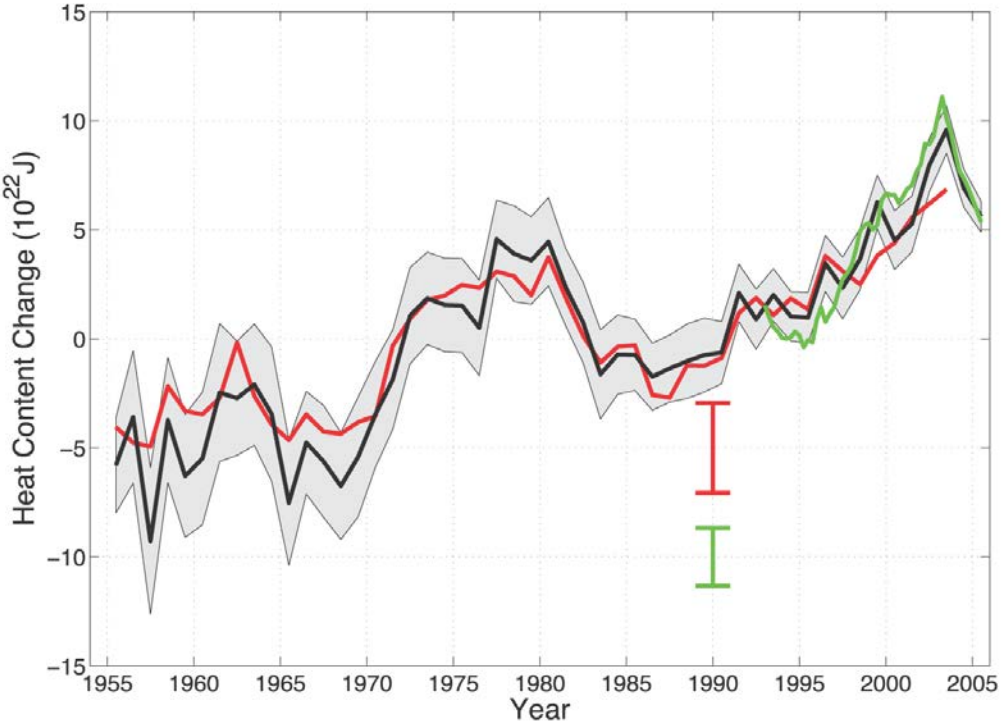

Figure 3.14. *Time series of global annual ocean heat content for the upper ocean (0 to 700 m depths). The black curve is updated from Levitus et al. (2005a), with the shading representing the 90% confidence interval. The red and green curves are updates of the analyses by Ishii et al. (2006) and Willis et al. (2004, depths of 0 to 750 m) respectively, with the error bars denoting the 90% confidence interval. The black and red curves denote the deviation from the 1961 to 1990 average and the shorter green curve denotes the deviation from the average of the black curve for the period 1993 to 2003 (Bindoff et al. 2007). IPCC.*

Increases in Pacific Ocean temperature are spatially variable. At 40° N (0-350 m depth) and at the equator (~ 250 m depth), temperatures have cooled whereas over the remaining North Pacific, trends indicate warming (IPCC 2007; see box Scale Dependency of Climate Change: Seawater Temperature). Warming at equatorial surface waters and cooling of waters at depth indicate a relaxation of the tropical thermocline (McPhaden and Zhang 2002). Notably, warming in North Pacific waters is not restricted to the surface (0-300 m), but can be observed to 3000 m water depth (Levitus et al. 2000).

Scale Dependency of Climate Change: Seawater Temperature

From 1961 to 2003 the global oceans have warmed by 0.10°C from the surface to a depth of 700 m (Bindoff et al. 2007). However, as seen with sea level rise, ocean warming is not consistent in space. In the Pacific Ocean, a large swath of cooling exists from the surface to 400 m depth along 40°N (heat content is proportional to temperature; Bindoff et al. 2007; Fig. 3.15). The regions depicted by blue in Figure 3.15 indicate cooling that is consistent with the positive phase of the PDO (via a strengthening of the Aleutian low). Again, different warming trends are obtained for data from different regions (or different time periods).

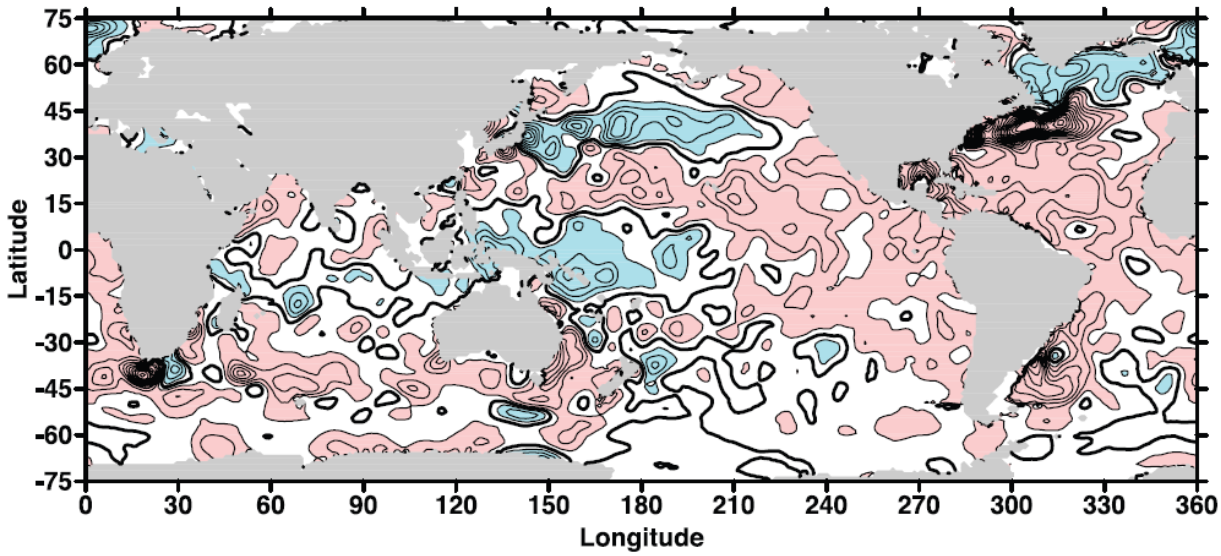

Figure 3.15. *Linear trends (1955–2003) of change in ocean heat content per unit surface area (W m^{-2}) for the 0 to 700 m layer, based on the work of Levitus et al. (2005). The linear trend is computed at each grid point using a least squares fit to the time series at each grid point. The contour interval is 0.25 W m^{-2}. Red shading indicates values equal to or greater than 0.25 W m^{-2} and blue shading indicates values equal to or less than –0.25 W m^{-2}. Adapted from Bindoff et al. (2007).*

Similarly, while large-scale studies show an increase in sea-surface temperature (SST) over the eastern Pacific Ocean (Fig 3.15), other results show a slow warming rate or decrease in SST in coastal waters (Bakun 1990; Mendelssohn and Schwing 2002; Garcia-Reyes and Largier 2010) due to an increase in wind-driven upwelling (see 3.3.3 Coastal Upwelling). Further, unpublished data suggest SST is increasing in sheltered nearshore waters and enclosed bays. So different SST trends will be obtained depending on the spatial scale of analyses.

Coastal measurements of sea surface temperature from Southern California to Oregon document an increasing trend in temperature offshore and at shore stations since these data were first collected in 1955 (McGowan et al. 1998; Enfield and Mestas-Nunez 1999; Sagarin et al. 1999; Mendelssohn et al. 2003; Palacios et al. 2004). Also, anomalies detected at one site were generally correlated with other sites, suggesting that temperature increases in one area captured the thermal signal for a much greater region. At sites in Southern California, seawater temperature has increased by as much as 1.5°C since 1951 (Roemmich and McGowan 1995; McGowan et al. 1998). However, ocean temperatures over the continental shelf off central California have exhibited cooling over the last 30 years (Mendelssohn and Schwing 2002; Garcia-Reyes and Largier 2010), consistent with an increase in coastal upwelling (see 3.3.3 Coastal Upwelling).

3.6.2 Ocean Acidification

The increased concentration of CO_2 in the ocean (due to rising atmospheric CO_2 concentrations) has impacted the chemistry (pH) and biology of the oceans (Feely et al. 2008). The impact of ocean acidification is a recent but major concern and has been described as the "other CO_2 problem" (Doney et al. 2009).

Increased CO_2 in the atmosphere (CO_{2atm}) leads to a reduction in ocean pH and a decline in the carbonate ion concentration (CO_3^{2-}) resulting in what has been termed "ocean acidification" (Caldeira and Wickett 2003). In the ocean, this carbonate system is controlled by chemical reactions in equilibrium, and the relative proportions of the three forms of dissolved inorganic carbon (DIC) affect seawater pH (a measure of the concentration of the hydrogen ion H^+), as follows:

$$CO_{2atm} \leftrightarrow CO_{2aq} + H_2O \leftrightarrow H_2CO_3 \leftrightarrow H^+ + HCO_3^- \leftrightarrow 2H^+ + CO_3^{2-}$$

The exchange of atmospheric carbon dioxide (CO_{2atm}) across the air-sea interface equilibrates surface seawater CO_2 with the atmosphere. This dissolved (aqueous) CO_2 reacts with seawater to form carbonic acid (H_2CO_3). Carbonic acid readily dissociates to hydrogen (H^+), bicarbonate (HCO_3^-), and carbonate (CO_3^{2-}) ions (see equation above). The relative proportions of these forms of dissolved inorganic carbon (DIC) in an ocean of pH 8.1 are 86.5% bicarbonate, 13% carbonate, and 0.5% dissolved CO_2 (Zeebe and Wolf-Gladrow 2001). Rising CO_{2atm} concentrations force a corresponding increase in H_2CO_3, a weak acid, resulting in increased hydrogen ion concentrations ($[H^+]$), which leads to a decrease in pH, and decreased carbonate ion concentrations. Figure 3.16 illustrates the increase in oceanic pCO_2 and the resulting decrease in pH since the mid-1980s at three time series stations. The pH levels at these stations have decreased 0.02 unites per decade, and globally, the average surface ocean pH has decreased by 0.1 units since pre-industrial times (Doney et al. 2009).

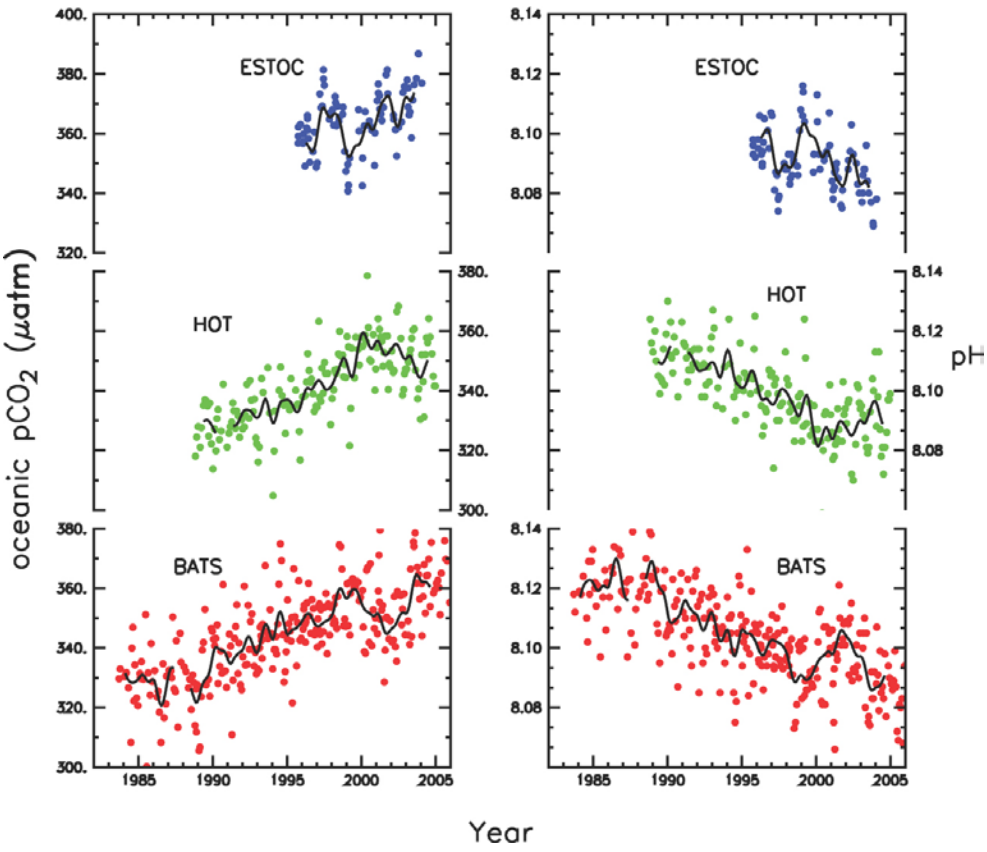

Figure 3.16. *Changes in surface oceanic pCO2 (left; in ìatm) and pH (right) from three time series stations: Blue: European Station for Time-series in the Ocean (ESTOC, 29°N, 15°W; Gonzalez-Dávila et al. 2003); green: Hawaii Ocean Time-Series (HOT, 23°N, 158°W; Dore etal., 2003); red: Bermuda Atlantic Time-series Study (BATS, 31/32°N, 64°W; Bates et al. 2002;Gruber et al. 2002). Values of pCO2 and pH were calculated from DIC and alkalinity at HOT and BATS; pH was directly measured at ESTOC and pCO2 was calculated from pH and alkalinity. The mean seasonal cycle was removed from all data. The thick black line is smoothed and does not contain variability at periods less than half a year (IPCC 2007).*

Carbonate ion is essential to the formation of calcium carbonate minerals (e.g., calcite and aragonite) that make up the shells and skeletons of many marine taxa (Orr et al. 2005, Fabry et al. 2008; Doney et al. 2009). Calcium carbonate becomes more soluble with decreasing temperature and increasing pressure (i.e., ocean depth). Calcium carbonate formation and dissolution rates also vary with saturation state (Ω), which depends on the concentrations of calcium and carbonate ions in seawater. Saturation states are typically highest in the tropical oceans, and begin to decrease with increasing latitude and decreasing temperature (Feely et al. 2004). A natural boundary, the saturation horizon, develops in seawater as a result of these variables, and this boundary delineates a depth of seawater above which carbonate minerals can form, but below which they dissolve if unprotected (Feely et al. 2004). The majority of marine organisms that produce shells and skeletons live above the saturation horizon, but increasing CO_2 levels are elevating the saturation horizon closer to the surface (Feely et al. 2004). Therefore increases in surface ocean CO_2 could have severe consequences for organisms that utilize external shells and skeletons.

A recent study by Feely et al. (2008) shows that pH is very low in upwelled waters in the study region and along the coast of western North America. In spring 2007, in a strong upwelling area off the northern California coast, the entire shelf up to the 50 m bottom contour became under-saturated with respect to aragonite ($\Omega_{arag} < 1.0$) and had a pH < 7.75 concomitant with intense upwelling (Fig. 3.17). These conditions at the ocean surface are not expected to occur elsewhere in the oceans until the year 2050 (IPCC 2007), but it is expected that similar conditions elsewhere along the northern and central California coast and in other strong upwelling systems will display this signal (Feely et al. 2008). While aragonite saturation and precision pH measurements are not often obtained, CO_2 levels over 1000 ppm have been observed during intense upwelling near Point Reyes and values just less than 1000 ppm have been observed near the surface at a number of other locations in the Arena-Reyes upwelling center (Vander Woude et al. *in preparation*). While monitoring changes in pH is still in its infancy and thus difficult to precisely quantify, these processes are expected to adversely influence any organism that produces calcium carbonate shell due to the decrease of pH and carbonate ion concentration (see 5.3 Invertebrates).

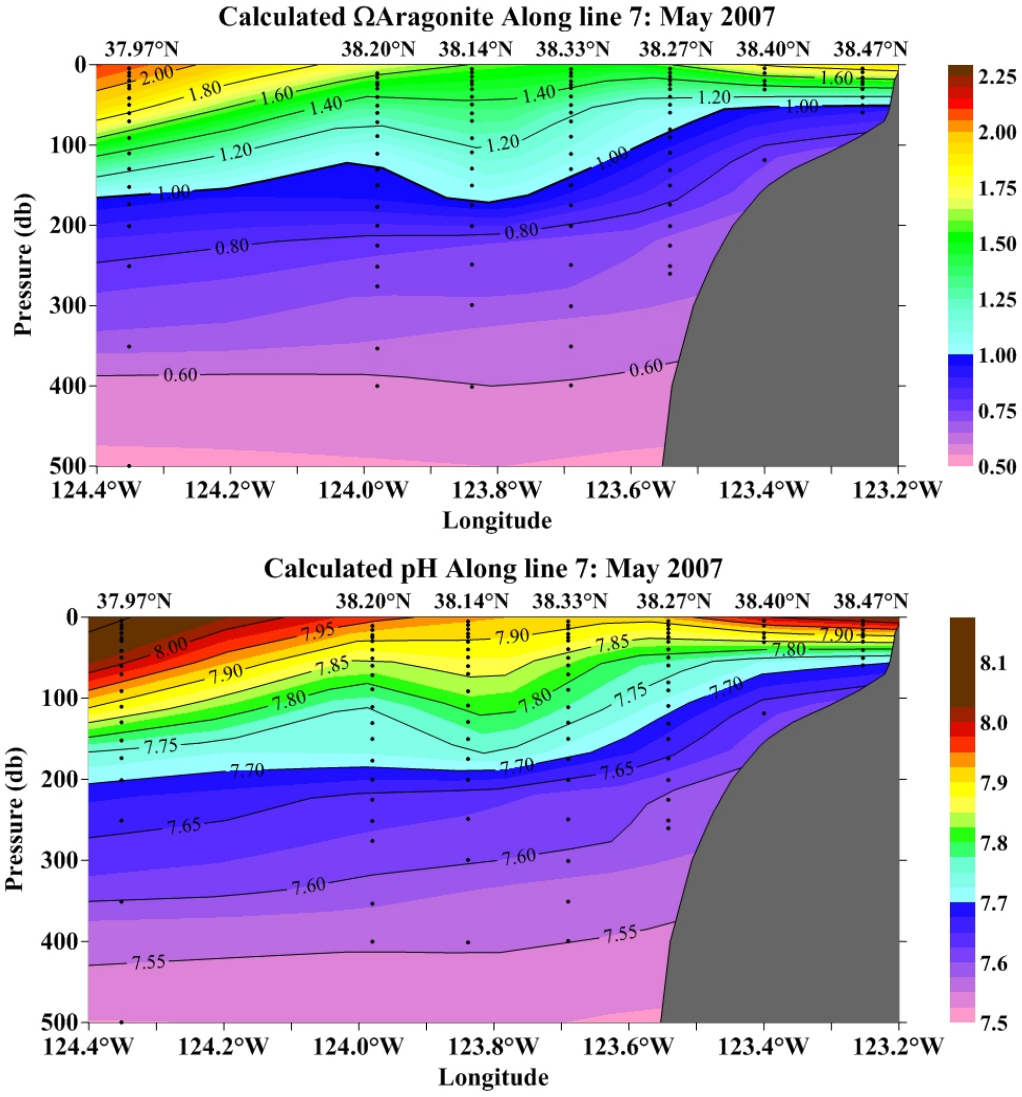

Figure 3.17. *(Top) Aragonite saturation state along transect line 7 (beginning just north of San Francisco Bay). (Bottom) pH values along transect line 7. Results calculated from May 2007 North American Carbon Program (NACP) West Coast Cruise along the continental shelf of western North America. Courtesy of D. Feely and D. Greeley / NOAA.*

Ocean acidification may also be driven by increases in freshwater input (low pH, low calcium) to estuarine habitats from rivers and streams, which decreases aragonite and calcite saturation state. Increases in freshwater have been projected by forecast models of global warming scenarios for California (Snyder and Sloan 2005). For example, Tomales Bay receives freshwater input from two creeks. During the upwelling season (approximately April to August), Tomales Bay becomes hypersaline, especially at the head of the bay (Hearn and Largier 1997; Largier et al. 1997), whereas in winter, sporadic heavy rains can induce low salinities. Runoff and tidal processes control ocean-estuary exchange, and therefore also control blooms of phytoplankton that alter seawater alkalinity and influence ocean pH and CO_2 concentrations. In a reanalysis of data from Smith and Hollibaugh (1997) it has been shown that aragonite saturation state (Ω) was critically low at the head of the bay during four winters, when freshwater input from Lagunitas Creek was greatest (Russell et al. *in preparation*). These processes may increase as northern California experiences changes in winter storms and rainfall in the future.

3.6.3 Salinity

Salinity is a key variable that is useful for detecting changes in precipitation, evaporation, runoff, ice melt, and ocean circulation (IPCC 2007). Detection of long term trends in ocean salinity is hampered by data deficits in some areas. Nonetheless, existing global salinity data indicate trends of freshening seawater at subpolar latitudes and increased salinity at tropical and subtropical locations. In the Pacific Ocean, increased precipitation as well as greater runoff and ice melt has resulted in decreased salinity at high latitudes. While Pacific subtropical regions have increased in salinity over time as a result of strong evaporation (IPCC 2007), overall, the Pacific Ocean basin has decreased in salinity (Boyer et al. 2005). CalCOFI data from Southern California indicate a long-term freshening of surface waters associated with decreased mixing of deep saline waters caused by persistent heating of surface waters (McGowan et al. 1998). Additionally, time series measurements indicate that freshening events in Southern California are associated with ENSO episodes and increased impact of subarctic water reaching the California coast in recent years (Gomez-Valdez and Jeronimo 2009). Few data are available that address Northern California sites specifically, but it is expected that similar processes would control salinity in this region. Salinities in coastal California will also be impacted by local-scale changes in precipitation and runoff, which is likely to include increases in precipitation during spring months (Snyder and Sloan 2005).

3.6.4 Nutrients

Ocean nutrient concentrations are affected by a variety of processes that have potential links to anthropogenic climate change. However, only a few studies (see Bindoff et al. 2007) exist within the Northeast Pacific that examine long term changes in macro-nutrient concentrations (e.g., nitrate, nitrite, phosphate, silicic acid). Perhaps less even is known about micro-nutrients in the CCE (e.g., iron, zinc). Generally, increased temperature and stratification should act to decrease the mixed layer depth, resulting in the upwelling of warmer nutrient poor waters. However, this is complicated by changes in wind structure and the magnitude of wind stress curl, as well as overall changes in upwelling intensity (see 3.1 Atmosphere and 3.3.3 Coastal Upwelling). Recent work on CalCOFI and Alaskan Gyre Line P datasets has documented a relationship between nutrients and upwelling and the North Pacific Gyre Oscillation (NPGO), suggesting a potentially useful index for measuring changes in long-term nutrient dynamics (Di Lorenzo et al. 2008; 2009). In coastal areas near rivers and estuaries, nutrient concentrations will be linked to precipitation patterns and the subsequent sediment and nutrient plumes created from freshwater

input. Because nutrient concentrations can have such a large effect on primary productivity and overall food web function, more studies are needed to determine how climate change will affect nutrients in the CCE.

3.6.5 Dissolved Oxygen

Dissolved oxygen (DO) concentrations in the ocean are dependent on a number of physical and biological processes, including circulation, ventilation, air-sea exchange, production and respiration (Keeling and Garcia 2002; Deutsch et al. 2005; Bograd et al. 2008). Climate-driven changes in any of these processes can result in significant changes in DO. Models driven by increasing greenhouse gases predict a decline in midwater oceanic DO, primarily as a result of enhanced stratification and reduced ventilation (Sarmiento et al. 1998; Keeling and Garcia 2002).

An extensive oxygen minimum zone (OMZ) exists along the continental margin of North America, within the California Current Ecosystem (CCE). Recent observations within the CCE have revealed significant reductions in DO in several locations, suggesting climate-driven variations in the processes controlling DO concentrations and a potential shoaling of the OMZ (Whitney et al. 2007; Bograd et al. 2008; Chan et al. 2008; Stramma et al. 2008). On the Oregon continental shelf, there has been an increase in the frequency and severity of hypoxic events and the novel rise of water-column anoxia, with accompanying high mortality of demersal fish and benthic invertebrate communities (Grantham et al. 2004; Chan et al. 2008). These events are seasonal and have been attributed to fluctuations in the intensity of upwelling, the DO content of upwelled water, and productivity-driven increases in coastal respiration (Wheeler et al. 2003; Grantham et al. 2004; Chan et al. 2008).

In the southern CCE, anoxic events have generally been limited to the deepest part of the submarine basins within the borderlands off southern California (e.g., Santa Barbara Basin, Berelson 1991; Kennett and Ingram 1995; Bograd et al. 2002). Differences in shelf bathymetry may make productivity-driven anoxic events less common off California relative to Oregon. However, hydrographic data collected on CalCOFI cruises have revealed significant declines in water-column DO throughout the southern CCE (Bograd et al. 2008). The largest relative DO declines occurred below the thermocline (mean decrease of 21% between 1984-2006 at 300 m), with significant linear trends at the majority of CalCOFI stations down to 500 m (the deepest depth sampled). The spatial pattern of the DO trends suggests that the advection of low-DO waters into the region (e.g., from the eastern tropical Pacific via the California Undercurrent) may have been a major contributor to the observed DO decline. Similar DO declines have been observed from the long-term Line P dataset extending from the southern tip of Vancouver Island out to the central Gulf of Alaska (Whitney et al. 2007). The CCE observations are also consistent with the observation of an expanding OMZ in the tropical Pacific, which is a source of deep waters to the CCE (Stramma et al. 2008). It should be noted, however, that there is a lack of historical DO observations from the central CCE (e.g., between Monterey Bay, CA and Cape Blanco, OR), revealing a significant data gap.

A decline in mid-ocean DO concentrations can be viewed as a vertical expansion of the OMZ, which may then impact a larger portion of the California Current shelf and slope regions. In the southern CCE, the hypoxic boundary (~60 μmol kg^{-1}) shoaled between 1984-2006 by an average of 40 m, and up to 90 m over the continental slope/shelf (Bograd et al. 2008). This expansion of the oxygen minimum layer could lead to cascading effects on benthic and pelagic ecosystems,

including habitat compression and community reorganization (Diaz and Rosenberg 1995; Childress and Seibel 1998; Levin 2003; Prince and Goodyear 2006; Bograd et al. 2008), range expansion of some organisms such as Humboldt squid (Gilly et al. 2006), as well as increased ocean acidification as low-DO waters are upwelled (Feely et al. 2008). Continued monitoring within the CCE, and particularly in the study region, is essential to understand the mechanisms and mitigate the ecological consequences of climate-driven changes in oceanic oxygen content.

Marine Sanctuaries Conservation Series ONMS-11-04

Climate Change Impacts: Gulf of the Farallones and Cordell Bank National Marine Sanctuaries

Report of a Joint Working Group of the Gulf of the Farallones and Cordell Bank National Marine Sanctuaries Advisory Councils

U.S. Department of Commerce
National Oceanic and Atmospheric Administration
National Ocean Service
Office of Ocean and Coastal Resource Management
Office of National Marine Sanctuaries

August 2011

Climate Change Impacts: Gulf of the Farallones and Cordell Bank National Marine Sanctuaries

Report of a Joint Working Group of the Gulf of the Farallones and Cordell Bank National Marine Sanctuaries Advisory Councils

John Largier
Bodega Marine Laboratory
University of California, Davis

Brian Cheng
Bodega Marine Laboratory
University of California, Davis

Kelley Higgason
Gulf of the Farallones National Marine Sanctuary
Office of National Marine Sanctuaries

U.S. Department of Commerce
John Bryson, Secretary

National Ocean and Atmospheric Administration
Jane Lubchenco, Ph.D.
Under Secretary of Commerce for Oceans and Atmosphere

National Ocean Service
David M. Kennedy, Assistant Administrator

Office of National Marine Sanctuaries
Daniel J. Basta, Director

Silver Spring, Maryland
August 2011

Disclaimer

Report content does not necessarily reflect the views and policies of the Office of National Marine Sanctuaries or the National Oceanic and Atmospheric Administration, nor does the mention of trade names or commercial products constitute endorsement or recommendation for use.

Report Availability

Electronic copies of this report may be downloaded from the Office of National Marine Sanctuaries web site at http://sanctuaries.noaa.gov. Hard copies may be available from the following address:

National Oceanic and Atmospheric Administration
Office of National Marine Sanctuaries
SSMC4, N/ORM62
1305 East-West Highway
Silver Spring, MD 20910

Cover

1) Wave breaking at Maverick's, Half Moon Bay, CA. Josh Pederson / SIMoN NOAA; 2) Krill: *Euphausia pacifica*. Matt Wilson/Jay Clark, NOAA NMFS AFSC; 3) Bottlenose Dolphins: *Tursiops truncatus*. NMFS Southwest Fisheries Science Center.

Suggested Citation

Largier, J.L, Cheng, B.S., and Higgason, K.D., editors. 2010. Climate Change Impacts: Gulf of the Farallones and Cordell Bank National Marine Sanctuaries. Report of a Joint Working Group of the Gulf of the Farallones and Cordell Bank National Marine Sanctuaries Advisory Councils. Marine Sanctuaries Conservation Series ONMS-11-04. U.S. Department of Commerce, National Oceanic and Atmospheric Administration, Office of National Marine Sanctuaries, Silver Spring, MD. 121 pp.

Contact

Kelley Higgason
Gulf of the Farallones National Marine Sanctuary
991 Marine Dr., The Presidio
San Francisco, CA 94129
415-561-6622 ext. 202
kelley.higgason@noaa.gov

Contributors

Josh Adams, United States Geological Survey
Sarah Allen, Point Reyes National Seashore
Dane Behrens, University of California, Davis; Bodega Marine Lab
Steven Bograd, National Marine Fisheries Service
Russell Bradley, PRBO Conservation Science
Bob Breen, Gulf of the Farallones National Marine Sanctuary Advisory Council
Brian Cheng, Gulf of the Farallones and Cordell Bank national marine sanctuaries; UC Davis
James Cloern, United States Geological Survey
Jeffrey Dorman, University of California, Berkeley
Jenifer Dugan, Marine Science Institute, University of California, Santa Barbara
Meredith Elliot, PRBO Conservation Science
Marisol Garcia-Reyes, University of California, Davis; Bodega Marine Lab
Brian Gaylord, University of California, Davis; Bodega Marine Lab
Mike Graham, Moss Landing Marine Laboratories
Edwin Grosholz, University of California, Davis; Bodega Marine Lab
Daphne Hatch, Golden Gate National Recreation Area
Annaliese Hettinger, University of California, Davis; Bodega Marine Lab
Kelley Higgason, Gulf of the Farallones National Marine Sanctuary
Tessa Hill, University of California, Davis; Bodega Marine Lab
Julie Howar, PRBO Conservation Science
Jaime Jahncke, PRBO Conservation Science; CBNMS Advisory Council
Heather Kerkering, Central and Northern California Ocean Observing System
Judith Kildow, Ocean Economics Program
Raphael Kudela, University of California, Santa Cruz
John Largier, University of California, Davis; Bodega Marine Lab; GFNMS Advisory Council
Lance Morgan, Marine Conservation Biology Institute; CBNMS Advisory Council
Kerry Nickols, University of California, Davis; Bodega Marine Lab
Tim Reed, Gulf of the Farallones National Marine Sanctuary
David Revell, Philip Williams and Associates
Karen Reyna, Gulf of the Farallones National Marine Sanctuary
David Reynolds, National Weather Service
Jan Roletto, Gulf of the Farallones National Marine Sanctuary
Jennifer Roth, PRBO Conservation Science
Mary Jane Schramm, Gulf of the Farallones National Marine Sanctuary
Frank Schwing, National Marine Fisheries Service
William Sydeman, Farallon Institute
John Takekawa, United States Geological Survey
Sage Tezak, Gulf of the Farallones National Marine Sanctuary
Pete Warzybok, PRBO Conservation Science

Authors

CHAPTER 1	
	Kelley Higgason
CHAPTER 2	
	Kelley Higgason, Brian Cheng
CHAPTER 3	
3.0	*Brian Cheng, Frank Schwing*
3.1	*Marisol Garcia-Reyes, David Reynolds, Frank Schwing*
3.1.1	*Marisol Garcia-Reyes, David Reynolds, Frank Schwing*
3.1.2	*Brian Cheng, David Reynolds*
3.1.3	*Brian Cheng, David Reynolds*
3.2	*Dane Behrens, Brian Cheng*
3.3	*Frank Schwing, David Reynolds*
3.3.1	*Frank Schwing, David Reynolds*
3.3.2	*Dane Behrens, Brian Cheng, David Revell, David Reynolds*
3.3.3	*Marisol Garcia-Reyes, Frank Schwing, John Largier*
3.3.4	*John Largier*
3.4	*David Revell, Frank Schwing*
3.5	*David Revell*
3.6.1	*Brian Cheng, Frank Schwing*
3.6.2	*Annaliese Hettinger, Tessa Hill*
3.6.3	*Brian Cheng*
3.6.4	*Brian Cheng, Raphael Kudela*
3.6.5	*Steven Bograd*
CHAPTER 4	
4.1	*Brian Cheng*
4.2	*Brian Cheng*
4.3	*Jennifer Roth, Jaime Jahncke*
4.4	*Brian Cheng, Jeffery Dorman*
4.5	*Brian Cheng*
CHAPTER 5	
5.1	*William Sydeman, Raphael Kudela*
5.2	*Brian Cheng, Mike Graham*
5.3	*Bob Breen, Brian Cheng*
5.4	*Brian Cheng*
5.5	*Jennifer Roth, Jaime Jahncke*
5.6	*Sarah Allen*
CHAPTER 6	
6.1	*Meredith Elliott, Jaime Jahncke, Frank Schwing*
6.2	*Lance Morgan*
6.3	*Pete Warzybok, Jaime Jahncke*
6.4	*Jenifer Dugan, David Revell*
6.5	*Brian Cheng, Brian Gaylord*
6.6	*Kerry Nickols, Mike Grahm, Brian Gaylord*